Khazar Journal of Science and Technology Volume 5 №2 2021, 49-70

DOI: 10.5782/2520-6133.2021.5.2.49

Brain Tumor Segmentation Methods based on MRI images: Review Paper

Behnam Kaini Kalejahi[1*], Sebalan Danishvar[2], Jala Guluzade[1]

[1]*Faculty of Engineering and Applied Sciences, Khazar University, Azerbaijan*

[2]*College of Engineering, Design and Physical Sciences*

[*]Corresponding author: bkiani@khazar.org

Abstract

Statistically, incidence rate of brain tumors for women is 26.55 per 100,000 and this rate for men is 22.37 per 100,000 on average. The most dangerous occurring type of these tumors are known as Gliomas. The form of cancerous tumors so-called Glioblastomas are so aggressive that patients between ages 40 to 64 have only a 5.3% chance with a 5-year survival rate. In addition, it mostly depends on treatment course procedures since 331 to 529 is median survival time that shows how this class is commonly severe form of brain cancer. Unfortunately, a mean expenditure of glioblastoma costs 100,000$. Due to high mortality rates, gliomas and glioblastomas should be determined and diagnosed accurately to follow early stages of those cases. However, a method which is suitable to diagnose a course of treatment and screen deterministic features including location, spread and volume is multimodality magnetic resonance imaging for gliomas. The tumor segmentation process is determined through the ability to advance in computer vision. More precisely, CNN (convolutional neural networks) demonstrates stable and effective outcomes similar to other automated methods in terms of tumor segmentation algorithms. However, I will present all methods separately to specify effectiveness and accuracy of segmentation of tumor. Also, most commonly known techniques based on GANs (generative adversarial networks) have an advantage in some domains to analyze nature of manual segmentations..

Keywords: Generative adversarial networks, Brain Tumor, Segmentation, Medical Images. **Introduction**

Today, three major categories can explain brain tumor segmentation based on different principles and degree of human interaction requirements. These include semi-automatic, fully automatic and manual segmentations (Pham et al., 2000). Firstly, semi-automatic brain tumor segmentation consists of software, interaction and user. The realization of tumor segmentation algorithms is a target area for software computing. The interaction covers the adjustment of segmentation information between the software and the user. For user case, it provides feedback response and visual information for software computing, but it requires to input some parameters before processes. Moreover, three processes of semi-automatic segmentation include feedback response, evaluation and initialization. One of the disadvantages of this segmentation category is to obtain same user at different times or different results from different experts. However, semi-automatic segmentation shows better results in comparison to manual segmentation. On the other hand, fully automatic brain tumor segmentation algorithm is a combination of prior knowledge and artificial intelligence. It is more likely to stimulate human intelligence to develop machine learning algorithms, but this method helps the computer analyze brain tumor segmentation without human interaction.

The manual brain tumor segmentation paints the regions of anatomic structure by using various labels and it draws the boundaries of brain tumor (Pham et al., 2000). In this case, anatomy as a representation of brain tumor images should be studied by brain tumor experts, but most of the time manual segmentation yields poor results due to error-prone and time-consuming issues. This is because the more brain tumor images in the clinic are emerging, the more errors occur for the experts. The solutions are semi-automatic and fully automatic segmentation methods which address such problems directly in an advanced way. In contact, these two segmentation methods exhibit partial-volume effects and irregular boundaries with discontinuities for tumor images. Currently, alternative three categories are proposed through MRI-based methods for brain tumor segmentation in order to solve challenges faced by semi-automatic and fully automatic brain tumor segmentation images.

1. Segmentation Methods

2.1. Classification and clustering methods

Due to the practice of radiology by radiologists, making accurate decisions and learning patterns from empirical data or learning complex relationship can be studied by providing machine learning which simplifies the diagnosis and anaylsis for medical images (Duda et al., 2012). In medical practice, unsupervised, semi-supervised and supervised learning are essential categories of classification and

clustering methods based on different principles and utilization of labels of training samples (Bishop et al., 2006), (Mitchell et al., 2006). Unsupervised learning algorithm contains no label information and only one set of observations for each sample (Alpaydin et al., 2004). Obviously, latent variables and a set of unobserved variables cause such features and observations. The main objective of the unsupervised learning is to reveal the latent variables and to determine relationship between samples between samples and behind the observations respectively (Hastie et al., 2005). Hence, clustering algorithm explains unsupervised learning effectively. Semi-supervised learning explores a combination of unsupervised and supervised learning algorithms (Chapelle et al., 2006). Due to having high costly labeling of data and being inapplicable for some applications semi-supervised learning was targeting the development of its algorithms (Christakou et al., 2005). Indeed, it has an advantage in terms of using unlabeled and labeled data in the training process. In addition, supervised learning algorithms study two major parts which include output observations (called as effects) or labels and input observation (called as causes) or features. Supervised learning shows a functional relationship which is a set of numerical coefficients and equations from training data. This data generalizes given procedures to testing data so that classification algorithm effectively explains supervised learning as a representative method. Classification or clustering methods in brain tumor segmentation include k-means, Markov Random Fields (MRF), Support Vector Machines (SVM), Artificial Neural Networks (ANN), Fuzzy C-means (FCM) and Atlas-based.

2.2. FCM algorithms

Pattern recognition is commonly used area for FCM method which corresponds to each cluster center between the data point and the cluster on the basis of distance issue, but before it assigns membership to each data point. Getting high possibility of membership towards the cluster center depends how nearer the data is to the cluster center. Getting encouraging results of MR data, getting satisfactory results better than k-means algorithm and better for overlapped data set, assigning membership of data points to not only one cluster center in which most data point exclusively belongs to one cluster center not similar to k-means are significant advantages of FCM algorithm.

Brain tumor segmentation is divided into tissue classes which generate segmentation images in order to demonstrate neuropathological and neuroanatomic issues by generating contrast information from raw MR image data. Necrotic core, active cells and unsupervised FCM clustering algorithm used edema are included in these classes. Furthermore, the integration of multispectral histogram analysis and knowledge-based methods enables MRI images to determine segmentation of brain

tumor. Fuzzy clustering as a knowledge-based method is an alternative procedure for MRI images of brain tumor segmentations. It is also used to build the tumor shape based on 3-D connected components. in addition to fuzzy knowledge and modified seeded region growing, a segmentation method which is so-called Fuzzy Knowledge-based Seeded Region Growing (FKSRG) shows effective segmentation results for multispectral MR images compared to segmentation of functional MRU with Brain Automated Segmentation Tool (Lin et al., 2012).

The FCM is considered as an iterative algorithm which is very time-consuming clustering method. In fact, Fast Generalized FCM (FGFCM) and Bias-Corrected FCM (BCFCM) algorithms are major solutions to decrease possible execution time in advance. FGFCM clustering algorithms are considered as robust FCM framework for segmentation of brain tumor. While BCFCM is a time-efficient algorithm in terms of providing brain images with good quality segmentation. In this method, supporting virtual brain endoscopy is a process obtained effectively by this algorithm in order to better analyze brain tumor segmentation.

A modified FCM-based method determines fast and accurate segmentation aiming to decrease sensitivity issue of standard FCM algorithm. For that reason, this method was proposed for mixed noises including impulse, intensity non-uniformity and Gaussian noises. Moreover, this method uses context based dependent filtering technique to better realize gray and spatial level distances. In this case, first step is extraction of a scalar feature value through neighborhood of each pixel. The next procedure is an observation of enhanced FCM algorithm regarding histogram-based approach connected with clustering process. Most researchers study a neighborhood attraction concept depending on features and relative location of pixels in order to develop the performance of FCM algorithm. However, segmentation results depend on degree of attraction in which determination of this process is difficult to obtain in most cases. The Genetic Algorithm (GAs) and Particle Swarm Optimization (PSO) have been introduced to reach optimal solutions. PSO has no challenges in finding exact solutions while GAs shows low performance for this issue. While the determination of the optimum value for degree of attraction is practically achieved through the combination of PSO and GAs. In addition to segmentation of brain tumor, the combination of fuzzy c-means and k-means algorithms are essential to determine the stage and size of tumor accurately. In contrast to the manual segmentation, this combination offers reproducibility and accuracy with tumor tissue segmentation that reduces time for the improvement of segmentation.

2.3. Atlas-based algorithms

Atlas-based algorithm is used to register various images, guide segmentation of brain tissue, and restrict tumor location. It is also used for generative classification models and three major steps are included in this algorithm. First of all, the atlas and the patient are added to global correspondence by assistance of an affine registration. Second, a template is introduced for brain tumor regarding seeding of a synthetic tumor into brain atlas. Third, brain tumor growth and optical flow principles explain seeded atlas deformation (Cuadra et al., 2004). Furthermore, researchers examine the tissue model through defining probabilistic information and imposing spatial constraints depending on atlases. Moreover, Expectation Maximization (EM) method is introduced to modify an atlas from different MRI modalities knowing that the information about tumor location is linked to the modified atlas with patient-specific information. This procedure enables a probabilistic tissue model to be employed and brain tumor to be segmented. One of advantages of atlas-based methods is about better integration between domain knowledge and consideration of atlas-based segmentation. While it is challenging to account the variability of such prior information. In fact, lesion growth prior model shows radial expansion of lesion which comes from the starting point for brain atlas deformation. Obviously, this process results in better segmentation results of brain tumor by analyzing large space-occupying tumors. In a population, brain atlases contain averaging pre-segmented images which are equally constructed and these methods experience lower segmentation guidance capability and local inter-subject structural variability. In order to solve such problems a multi-region-multi-reference framework is a best alternative to consider for atlas-based neonatal segmentation of brain tumor. As a result of using a spatial regularization and generative probabilistic model, the combination of a latent brain tumor atlas and healthy brain atlas is an accurate determination of brain segmentation from multi-sequence images. The Figure 1 demonstrates the results of T1 and T2 brain tumor segmentation as a part of atlas-based segmentation of magnetic resonance brain images. The localization suggests multi-modal segmentation optic pathway gliomas to be used for classification with probabilistic tissue model based on brain atlas at a recent time (Weizman et al., 2012). The effectiveness and practicability of atlas-based methods have a close relationship with the precise atlas. In Table 1, Talairach-Tournoux, Whole Brain, BrainWeb, and Brodmann are examples for atlases described as follows:

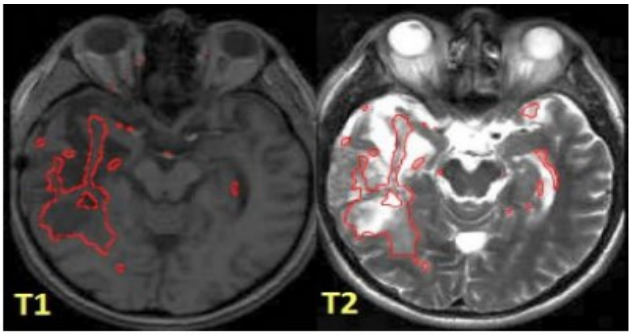

Figure 1. The results of T1 and T2 brain tumor segmentation

Table 1. Talairach-Tournoux, Whole Brain, BrainWeb, and Brodmann as an example

Name	Representation	References
Brodmann	The first brain atlas	Brodmann, 1909
Talairach-Tournoux	Construct a three-dimensional coordinate to provide a standard space	Talairach & Tournoux, 1988
BrainWeb	Widely used in the brain MRI images analysis	Evans et al., 1991
Whole Brain	Used in neurosurgery at Harvard Medical School	Shenton et al., 1995

2.4. MRF algorithms

These algorithms describe the integration of spatial information with classification or clustering process. Overlapping and effect of noise are possible issues that have been reduced by adding MRF in clustering methods. If the neighbor of labeled region is the same, MRF will determine this process by the fact that the region is strongly labeled (non-brain tumor or brain tumor) (Tran et al., 2005). Sequence data is labeled and segmented through building probabilistic models using Conditional Random Fields (CRF). Both MRF and CRF provide high accuracy for segmentation of brain tumor results by representing complex dependencies among data sets. GMM as an example of the mixture model can model different tissues including Necrotic Core (NC), Edema (E), GM, WM, Active Cells (AC) and CSF. This model uses Iterated Condition Modes (ICM) algorithm to train the MRF. Each tissue can be segmented by different models of different tissues. A multi-layer MRF framework can easily detect brain abnormalities so that such layers include input, structural coherence, region intensities, and spatial locations (Gering et al., 2002). Moreover, it is clear

that a change in high-level classification depends on a given voxel which is correlated with strong similarities shared by the attributes of lower-level layers. Spatial accuracy-weighted Hidden Markov random field and Expectation maximization (SHE) provides better quality of tumor segmentation in terms of enhanced-tumor and automated tumor segmentation (Nie et al., 2009). In clinical applications, high-resolution images are commonly determined together with low-resolution sequences. The process of tumor segmentation follows multi-channel MR images using different resolutions through incorporation of the optimization procedure of the Hidden MRF (HMRF) with the spatial interpolation accuracy of low-resolution images proposed by SHE (Bauer et al., 2011). Consequently, SHE algorithm presents more accuracy for the results of tumor segmentation. In case of an automatic method, brain tissues are segmented based on non-rigid registration of an average atlas which is combined with a biomechanically justified tumor growth model. It aims to detect causality of tumor mass-effect in a way to simulate soft-tissue deformations. Correspondence between the patient image and the atlas is the process provided by the tumor growth model which is considered and formulated as mesh-free MRF energy minimization problem before registration step. Compared to other approaches, tumor growth model is fast, simple and non-parametric due to maintaining similar accuracy. An automated hierarchical probabilistic framework supported through the use of an adapted MRF framework and multi-window Gabor filters enable brain tumors to be segmented from multispectral brain MRI (Subbanna et al., 2013). BraTS database in the framework assists segmentation of brain tumor as edema and non-edema. The Figure 2 shows how labels of algorithm correspond to labels of expert closely.

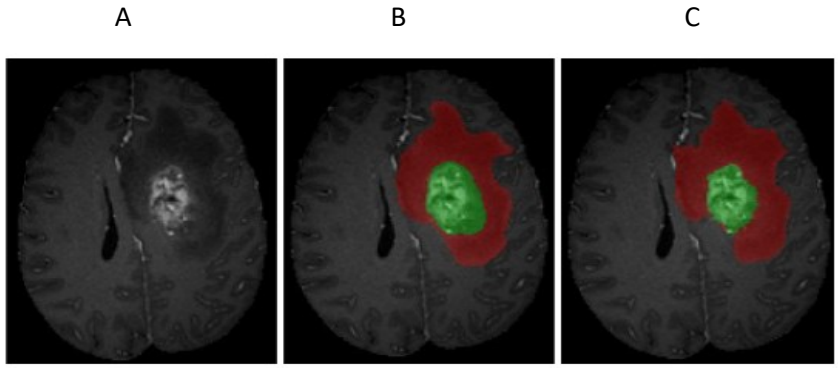

Figure 2. a) unlabeled TIC slice; b) expert labelling; c) algorithm labels (red – edema, green – non-edema)

2.5. SVM algorithms

Vladimir N. Vapnik invented the original version of SVM algorithm, but Cortes and Vapnik in 1993 studied current standard incarnation. To deal with supervised classification issues, a parametrically kernel-based method was proposed as SVM and brain tumor segmentation was a commonly known field for SVM algorithms. One-class SVM examines the ability to learn the nonlinear distribution of image data which uses no prior knowledge (Zhou et al., 2013). It is also applicable to achieve better segmentation results by following an implicit learning kernel and automatic procedure of SVM parameters training. These results support the extraction of brain tumors for better segmentation results compared to fuzzy clustering method. The researchers were willing to build voxel-wise intensity-based feature vectors via a high number of MRI modalities classified by SVM (Verma et al., 2008). The healthy tissues and also sub-compartments of healthy and tumor regions are segmented by this method, but similar approach based on SVM used a lower number of modalities and segmented one tumor region. The feature selection with kernel class was introduced to improve this method and it showed better results (Ruan et al., 2011). In order to segment the brain tumor from multi-sequence MRI images a fusion process and a multi-kernel based SVM in collaboration with a feature selection was offered as an alternative. Ameliorating the contour of tumor region (use of the distance and the maximum likelihood measures) and classification of tumor region (use of a multi-kernel SVM) are major two steps of a multi-kernel based SVM integrated with fusion and feature selection processes. In addition to classifying the tumor region, this step focuses on the performance of multi-image sources and multi-results. The accuracy and diminution of total error are expected results obtained through this method compared to traditional version of single kernel SVM. A fully automatic method was also essential to define segmentation of brain tissue which used multispectral intensities for SVM classification as a combination (Bauer et al., 2011). This method textured with hierarchical approach (specifically, subsequent hierarchical regularization) based on CRF to get acceleration and robustness. Thus, better results and accuracy can be achieved by different levels of regularization at various stages. The Figure 3 denoted potentially useful effects of SVM algorithms for MRI images in segmentation of brain tumor. The Table 2 explains the relatively good methods and their presentations of MRI-based brain tumor segmentation.

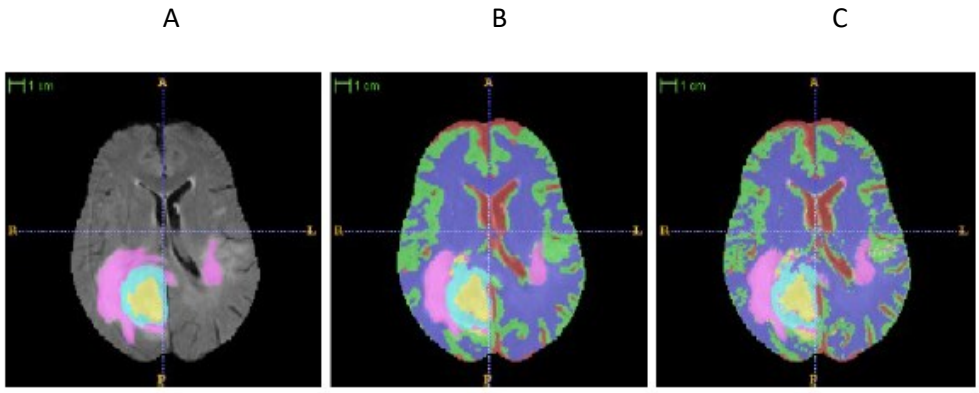

Figure 3. manual segmentation. a) hierarchical SVM-classification with CRF-regularization; b) non-hierarchical SVM-classification without regularization

Table 2. MRI-based brain tumor segmentation

Method	**Presentation**	**References**
Combination of k-means and fuzzy c-means	Better accuracy and reproducibility	Gupta et al., 2013
FKSRG	Lower over- and under-segmentation	Lin et al., 2012
Multi-region + multi-reference framework	Higher tissue overlaps rates and lower standard deviations	Shi et al., 2010
Generative probabilistic model + spatial regularization	Improvement over the traditional multivariate tumor segmentation (25 glioma)	Menze et al., 2010
Probabilistic model + localization	More robust applied to monitor disease progression	Weizman et al., 2012
Non-rigid registration + atlas + MRF	Multivariate tumor segmentation	Menze et al., 2010
SVM + CRF	10 multispectral patient datasets more detail segmentation low computation times	Bauer et al., 2011
Decision Forests + tissue-specific Gaussian mixture models	Segmenting the individual tissue types simultaneously such as AC, NC, E, etc.	Zikic et al., 2012
SVM + Kernel feature selection	Good results tested in T1w, T2w and T1c, low computation time	Zhang et al., 2011

2.6. Deformable model methods

Parametric and geometric deformable models are major components of model-based segmentation methods that can handle the issue of the appearance of 3-D MRI data

with respect to extraction of boundary elements which belong to same structure and integration of those elements into a consistent and coherent structure model (Lorenzo et al., 2013). In most cases, such issues are challenging to be segmented through simple methods compared with combination of SVM classification techniques which demonstrate high accuracy and diminution of total error. The capability of segmenting images of anatomic structures helps to determine resistance of deformable models. This segmentation exploits constraints about size, shape and location of anatomic structures which stem from image data with a prior knowledge. Deformable models are highly adjustable for the variability of biological structures in terms of various individuals. In addition to deformable models, they are more likely to assist clinicians and medical researchers through intuitive interaction mechanisms in order to determine necessary model-based image interpretation task.

2.7. Parametric deformable models

These models were so-called active contour models and snakes in some periods. After introduction of snakes in 1988, they are used to locate object contours including appropriate initialization in practice. The snakes are capable and sensitive to detect the boundary of brain tumors that is highly significant as a step of brain tumor segmentation in parametric deformable models. According to studies done about the resolution of the boundary, the snake technique shows more effective results compared to conventional edge detection including Canny, Sobel and Laplacian algorithms. However, the snake function in homogeneous regions is positively obtained while it is zero at the edges. Therefore, the improvement of brain tumor segmentation results on T1 brain tumor MRI was achieved using the balloon model and the Gradient Vector Flow (GVF). GCF aimed to analyze inability and short capture range which stem from the traditional snakes to track concavity of boundary. Moreover, the spatial relations as refinement step enable a parametric deformable model to estimate boundaries of any type of brain tumors accurately which is on T1 MRI (Gooya et al., 2011). The growth of snakes capture range can be defined by the balloon model apart from the parametric deformable model. The combination of deformable registration and segmentation of brain scans was proposed based on Expectation Maximization (EM) algorithm to a normal atlas in a way to explain incorporation of atlas seeding and a glioma growth model. This process studies modified atlas which represents the normal atlas into one with edema and a tumor. In addition, utilization of the posterior probability estimation of different tissue labels and registration into the patient space are essential characteristics of the modified atlas. The Expectation Maximization algorithm is highly optimistic to refine the posterior probabilities of tissue labels, the tumor growth model parameters and the estimates of registration parameters. It is also necessary to note that manual location of initial position of the parametric

deformable model demonstrates avoidance of converging to wrong boundaries if it is close to desired boundary.

2.8. Geometric deformable models

Geometric Deformable Models (GDM) is sometimes known as level sets which improves topological changes for merging of contours and splitting processes. In fact, these procedures are more challenging to be handled naturally in terms of topological changes when using segmentation of 3D MRI data through parametric deformable models. In most cases, segmentation methods of brain tumor cannot be easily achieved in practice when dealing with regularly shaped objects. On the other hand, the issue stems from improvement of initialization of parametric active contours and symmetrical placement of initial contour with respect to boundaries of interest. Level-set snakes were highly preferable to gain an advantage compared to mathematical morphology and conventional statistical classification, because snakes experience careful initialization which have constant propagation and leak through missing boundary parts. A knowledge-based segmentation algorithm combines level-set snakes and pixel-intensity distribution that present more precise boundaries. Some researchers examined a deformable model using a Charged Fluid Framework (CFF) to aim brain tumor segmentation for a certain period of time (Prastawa et al., 2004). However, CFF was extended and modified for brain tumor segmentation by proposing the Charged Fluid Model (CFM) (Chang & Valentino et al., 2006). Brain tumor can be segmented in a variable level set formulation by proposing a region-based active contour model (Li et al., 2008). This model suggested that the image intensities were approximated on two sides of contour by two fitting functions originated from data fitting energy. A regulation term as a part of the level set formulation shows derivation of a curve evolution which potentially targets energy minimization. The level set regularization term preserved regularity of level set function in a way to eliminate expensive re-initialization. In this case, the progress of level set function depends on accurate computation of the level set regularization term. A few researchers determined a local clustering criterion function which is specified for intensities considered in a neighborhood of each point (Li et al., 2011). However, a local intensity clustering property was also studied through brain tumor and other images with respect to intensity inhomogeneities. Integration of the local clustering criterion supports an energy functional over the neighborhood center in order to convert to formulation of the level set. Estimation of bias field and level set evolution with an interleaved process led to minimization of the energy (Hamamci et al., 2012). Combination of tumor segmentation and level set including tumor probability was achieved by a tumor-cut algorithm which resulted spatial smoothness.

To sum up, FCM, ANN and MRF are commonly used algorithms in terms of deformable model analysis. This method can aim the accuracy of brain tumor segmentation by incorporating two or more algorithms. Therefore, brain tumor segmentation has a direct effect on medical image analysis for surgical planning that is most important issue in term of validity of segmentation process. As a part of tumor segmentation, commonly applied evaluation standards include Dice Similarity Coefficient (DSC) and Jaccard coefficient which range from 0 indicating no overlap to 1 indicating perfect overlap (Crum et al., 2006). Moreover, probabilistic brain tumor segmentation was analyzed through three following validation metrics; Mutual Information (MI), Dice Similarity Coefficient (DSC) and the Receiver Operating Characteristic curve (ROC) (Archip et al., 2007). These methods aim to sustain tumor monitoring, a preliminary judgment on diagnosis as well as the physician with therapy planning.

2.9. Trilinear Interpolation Algorithm Techniques for 3D MRI Brain Image

There are many diagnoses and detection imaging techniques for treatment of potential risks caused by brain tumor diseases (Athertya & Poonguzhali, 2012). Computed Tomography (CT), Scanner, Position Emission Tomography (PET) and Magnetic Resonance Imaging (MRI) are commonly recognized diagnostic imaging tools to be practiced for tumor segmentation. In recent year, researches show that the process of obtaining 3D images from 2D medical images becomes increasingly necessary to determine an appropriate identity and regional development of tumors. Moreover, Machine Cube supports 2D CT image constructed 3D spine image or 3D surface of knee (Patel & Mehta, 2012). In this method, data blocks are divided into cubes that were made up of eight adjacent voxels. By using the triangular mesh material surfaces were constructed from there eight adjacent voxels. As a result, simple construction operations, 3D image production with high resolution and fast calculation are advantageous procedures experienced through this method. If the large number of 2D image data is processed, the calculation process slows down. In most cases, noise occurred due to images captured from sensor should be reduced by pre-processing 2D images in order to construct the 3D image with high quality of improvement. Therefore, a mean-unsharp filter is able to increase filtered noise and high frequency components. Before low-level image separation the intensity values of grayscale image may process the growth method of MRI images (Kumaran & Thimmiaraja, 2014). In this case, low-contrast images can be easily changed to higher-contrast images. Furthermore, making the tumor boundary depends on how morphological operations are utilized in order to stretch and fill a possible object for segmentation process. In this section, we will determine Otsu method for constructing 3D image with a support of segmentation of 2D images by finding the gray level threshold values.

On the other hand, segmentation method can be jointly connected with the algorithm of regional development with respect to similarity of adjacent pixels related to the nuclear point. Choosing the error and nuclear initial point which depend on between neighboring pixels and nuclear point can be defined as a result of combination of algorithm (Ho et al., 2016). Practically, the acquisition of 2D medical image may process noise on it, but Otsu technique as a threshold of traditional method segment some of the areas required for 3D image development. According to some research studies done on Otsu method, it may not often demonstrate better results. Instead, dividing 2D image into many layers by Otsu method with multilevel may provide better and efficient results. Pixels in 2D image are combined with region development algorithm to process segmentation of the image in which pixels have same regions (Zhang et al., 2016). The process may continue until the 2D image reaches coordinate axes (x, y, z) after segmentation. The calculation of approximate value of a point allows to construct the 2D image surface between two consecutive layers which are represented in the spatial domain. In fact, the linear interpolation approves this construction of 2D image surface before calculation of a value of the point (Hagan et al., 2009).

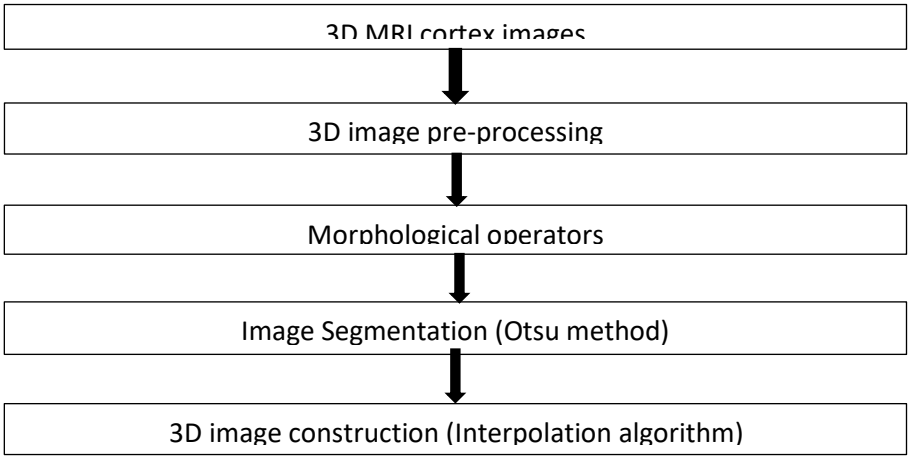

Figure 4**.** Otsu method or image segmentation

Figure 4. 3D image construction

Binh Duong General Hospital provided dataset for construction of 3D image by considering 44 2D MRI brain images with 256x192 pixels. There are some major following steps to describe the construction of 3D image from 2D MRI human cortex images. First step is to re-process 2D image including image enhancement and noise rejection. Second step is to employ morphological operator and eliminate pixels in 2D images around object boundaries. Third step is called Otsu method or image

segmentation where segmented and pre-processed images for 3D construction separate the brain area from the cortex. Final step is to construct 2D images after the segmentation to obtain 3D image by using a trilinear interpolation algorithm (also known as 3D image construction) figure 4.

2. Image pre-processing

Image pre-processing follows an average filter process to smooth 2D MRI images with noise in order to construct 3D image. The equation below describes elimination of noise by applying the average filter that is convoluted with each 2D MRI image.

$$r(x,y) = \frac{1}{ab} \sum_{s=-a}^{a} \sum_{t=-b}^{b} w(s,t) f(x+s, y+t)$$

- r(x,y) is output image after the process of filtering;
- w(s,t) is axb filter window.

In figure A, the average filter with a 3-by-3 kernel after convolution is given as the result of 2D MRI cortex image $\frac{1}{9}\begin{pmatrix} 1 & 1 & 1 \\ 1 & 1 & 1 \\ 1 & 1 & 1 \end{pmatrix}$.

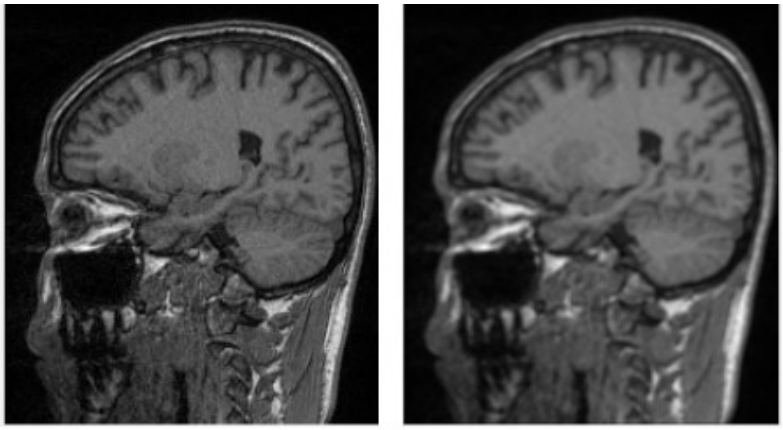

5- 1 5- 2

Figure 5. 5-1original human cortex image; 5-2 cortex image after the mean filter

After separation of complete brain region form the cortex image, the convoluted image provides smoother processing results in terms of using mean filter compared with using the median filter.

6-1 6-2

Figure 6. 6-1 image after using the mean filter; 6-2 image after using the median filter

In Figure C, not only enhancement of image with high frequency components but removal of low frequency components may be realized through application of unsharp filter with 3x3 size.

$$\frac{1}{2}\begin{pmatrix} -1 & 0 & -1 \\ 0 & 6 & 0 \\ -1 & 0 & -1 \end{pmatrix}$$

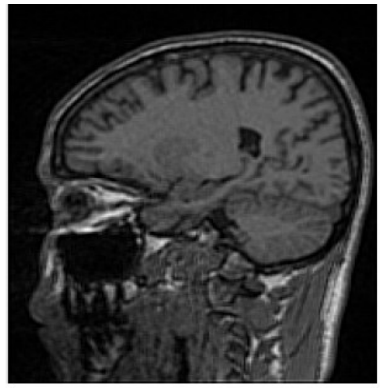

Figure 7. 2D MRI cortex image after the unsharp filter

Moreover, image enhancement is a solution to make object better on higher contrast in case of low contrast after image filtering. Spreading the pixel values in the image is a significant procedure to expect transformation of the higher contrast image when proposing a histogram equalization algorithm (Kaur & Rani, 2016). This algorithm uses a special equation to enhance the image as follows:

$$p_r(k) = \frac{n_k}{MN}$$

- nk is the number of pixels observed at the kth gray level in terms of the input image;
- MN is total pixels of the image;
- Pr(k) denotes the probability density function in the image connected with the kth gray level values.

Apart from probability density function (PDF), the calculation of the output expression of the image is defined:

$$s = (L-1)\sum_{j=0}^{k} p_r(j)$$

- L denotes the number of gray levels in the image;
- S(x,y) denotes the number of the pixels with respect to output image at the kth gray level.

In Figure D, first image represents before enhancement issue which uses unsharp filtering process. While, second image clearly shows after enhancement procedure. Nevertheless, the histogram equalization stimulates unsharp image with high frequency components to be enhanced for creation of higher contrast. Hence, figure 1 and 2 demonstrates representation of images where image before enhancement experiences the large number of pixels with distribution of being closed to the zero point. However, image after enhancement offers the histogram equalization with pixel values spreading on gray level axis.

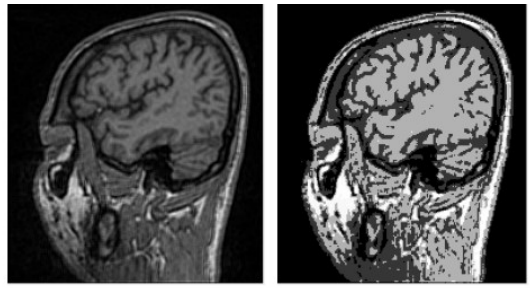

8-1 8-2

Figure 8. 8-1 image using the unsharp filter; 8-2 image after enhancement

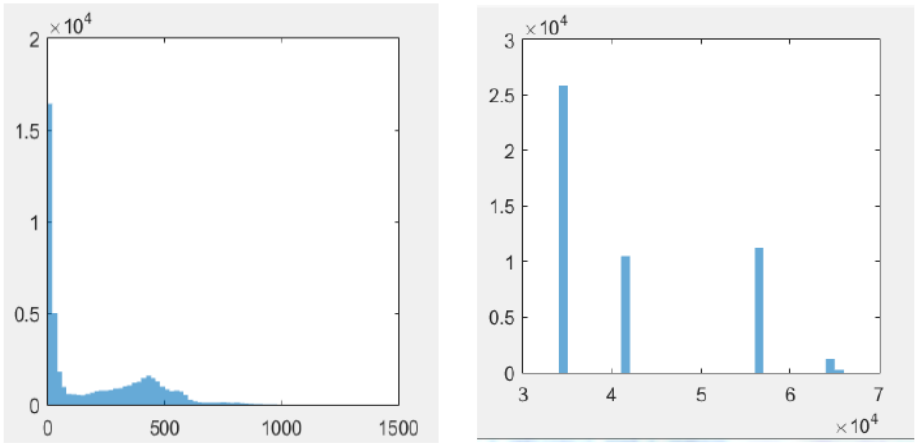

9-1 9-2

Figure 9. 9-1 image before enhancement; 9-2 image after enhancement using the histogram equalization

4. Morphological Operation

The enhanced image continues the process for image imperfection after filtering 2D MRI cortex image, but this filtering removes noise and enhances the image. As a result of the image enhancement, a morphological algorithm removes a few unnecessary parts around objects for the image. Only potentially important object is remained for 3D image construction by morphological algorithm. In addition, Dilation and Erosion are common operations of this algorithm in which the dilation operator considers structures and shapes of 2D image enhancement. At this moment, the morphological operation removes the undesired parts and combines boundaries around the objects (Sahar et al., 2016). On the other hand, the morphological image determines the convolution between a kernel and the input image for image calculation as given below:

$$m(x,y) = max\begin{cases} s(x-i,y-j) + h(i,j) \\ |(x-i),(y-j) \in D_s, (i,j) \in D_h \end{cases}$$

- h(i,j) is a kernel with the size of 2x2 matrix
- Ds and Dh are the domains of s image and k kernel.
- S(x-i,y-j) denotes output images.
- M(x,y) denotes input images.

In figure 10, the matrix of the 2x2 kernel is structured as follows:

1	1
1	1

Figure 10. matrix of the 2x2

In figure 11-2, the dilation operator in morphological algorithm enlarges the boundaries of object regions when producing the 2D MRI cortex image. For this reason, image after morphological operation combines the boundaries of object regions and provides better results compared with the enhanced image given as in figure 11-1.

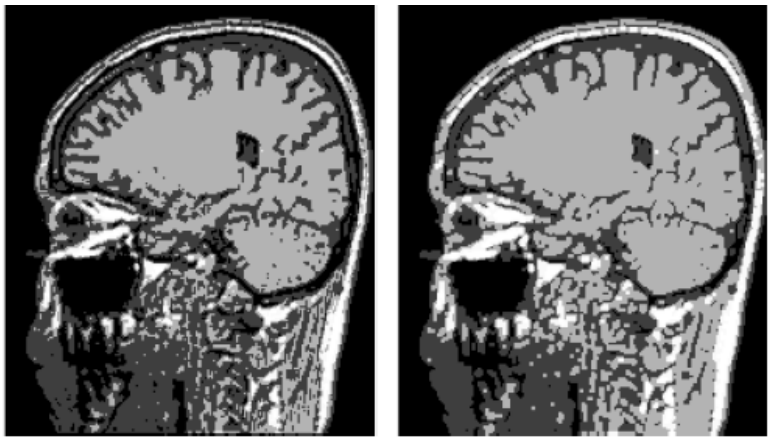

11-1 11- 2

Figure 11. 11-1 representation of the enhanced image; 11-2 Image after the morphological operation

References

Archip, N., Jolesz, F. A. & Warfield, **S. K.** (2007). A validation framework for brain tumor segmentation, Academic Radiology, vol. 14, no. 10, pp. 1242-1251.

Athertya, J. & Poonguzhali, S. (2012)."3D CT Image Reconstruction of the Vertebral Column", International Conference on Recent Trends in Information Technology, pp. 81 - 84.

Bauer, S., Nolte, L. P. & Reyes, M. (2011). Segmentation of brain tumor images based on atlas-registration combined with a markov-random-field lesion growth model, in

Biomedical Imaging: From Nano to Macro, 2011 IEEE International Symposium on, IEEE, pp. 2018-2021.

Bauer, S., Nolte, L. P. & Reyes, M. (2011). Fully-automatic segmentation of brain tumor images using support vector machine classification in combination with hierarchical conditional random field regularization, in Medical Image Computing and Computer-Assisted Intervention-MICCAI 2011. Springer, pp. 354-361.

Bishop, C. M. (2006). Pattern Recognition and Machine Learning, vol. 1. Springer New York.

Brodmann, K. (1909**).** Vergleichende Lokalisationslehre der Gro hirnrinde. Springer.

Cai, W., **Chen, S. & Zhang, D.** (2007). Fast and robust fuzzy c-means clustering algorithms incorporating local information for image segmentation, Pattern Recognition, vol. 40, no. 3, pp. 825-838.

Cai, H, **Verma, R, Ou, Y., Lee, S. K., Melhem, E. R. & Davatzikos, C.** (2007). Probabilistic segmentation of brain tumors based on multi-modality magnetic resonance images, in Biomedical Imaging: From Nano to Macro, 2007. ISBI 2007. 4th IEEE International Symposium on, IEEE, pp. 600-603.

Chapelle, O., **Schoellkopf, B. & Zien, A.** (2006). Semi-Supervised Learning, vol. 2. MIT Press Cambridge.

Chan, T. F. & Vese, L. A. (2001) Active contours without edges, Image Processing, IEEE Transactions on, vol. 10, no. 2, pp. 266-277.

Chang, H. H. & Valentino, D. J. (2006). Image segmentation using a charged fluid method, Journal of Electronic Imaging, vol. 15, no. 2, pp. 023011-023011.

Christakou, C., **Lefakis, L., Vrettos, S. & Stafylopatis, A.** (2005). A movie recommender system based on semi-supervised clustering, in Computational Intelligence for Modelling, Control and Automation, 2005 and International Conference on Intelligent Agents, Web Technologies and Internet Commerce, International Conference on, IEEE, vol. 2, pp. 897-903.

Cuadra, M. B, **Pollo. C, Bardera, A, Cuisenaire, O, Villemure, J. G. & Thiran, J. (**2004**).** Atlas-based segmentation of pathological mr brain images using a model of lesion growth, Medical Imaging, IEEE Transactions on, vol. 23, no. 10, pp. 1301-1314.

Crum, W. R, Camara, O. & Hill, D. L. (2006). Generalized overlap measures for evaluation and validation in medical image analysis, Medical Imaging, IEEE Transactions on, vol. 25, no. 11, pp. 1451-1461.

Duda, R. O., **Hart, P. E. & Stork, D. G.** (2012). Pattern Classification. John Wiley & Sons.

Evans. A, Marrett, S., Torrescorzo, J., Ku. S. & Collins. L. (1991). Mri-pet correlation in three dimensions using a volume of Interest (voi) atlas, Journal of Cerebral Blood Flow & Metabolism, vol. 11, pp. A69-A78.

Fletcher-Heath, L. M, **Hall, L. O., Goldgof, D. B. & Murtagh, F. R.** (2001). Automatic segmentation of non-enhancing brain tumors in magnetic resonance images, Artificial Intelligence in Medicine, vol. 21, no. 1, pp. 43-63.

Forouzanfar, M., **Forghani, N. & Teshnehlab, M. (**2010**).** Parameter optimization of improved fuzzy c-means clustering algorithm for brain mr image segmentation, Engineering Applications of Artificial Intelligence, vol. 23, no. 2, pp. 160-168.

Garc´ıa-Lorenzo, D., **Francis, S., Narayanan, S., Arnold. D. L. & Collins, D. L.** (2013). Review of automatic segmentation methods of multiple sclerosis white matter lesions on conventional magnetic resonance imaging, Medical Image Analysis, vol. 17, no. 1, pp. 1-18.

Gupta, M. P. & Shringirishi, M. M. (2013) Implementation of brain tumor segmentation in brain mr images using k-means clustering and fuzzy c-means algorithm, International Journal of Computers & Technology, vol. 5, no. 1, pp. 54-59.

Gooya, A., **Pohl, K. M., Bilello, M., Biros, G. & Davatzikos, C.** (2011). Joint segmentation and deformable registration of brain scans guided by a tumor growth model, in Medical Image Computing and Computer-Assisted Intervention-MICCAI 2011. Springer, pp. 532-540.

Hagan, R. (2009). "Numerical Methods for Isosurface Volume Rendering", Virginia Polytechnic.

Hamamci, A., Kucuk, N., Karaman, K., Engin, K. & Unal, G., Tumor-cut. (2012). Segmentation of brain tumors on contrast enhanced mr images for radiosurgery applications, Medical Imaging, IEEE Transactions on, vol. 31, no. 3, pp. 790-804.

Hastie, T., **Tibshirani, R., Friedman, J. & Franklin**, **J.** (2005). The elements of statistical learning: Data mining, inference and prediction, The Mathematical Intelligencer, vol. 27, no. 2, pp. 83-85.

Ho, Y., **Lin, W., Tsai, C., Lee, C. & Lin, Chih, Y.** (2016). "Automatic Brain Extraction for T1 – Weighted Magnetic Resonance Images Using Region Growing", International Conference on Bioinformatics and Bioengineering, pp. 250 - 253.

Kaur, H. & Rani, J. (2016). "MRI brain image enhancement using Histogram equalization Techniques", International Conference on Wireless Communications, Signal Processing and Networking, pp. 770 - 773.

Kumaran, N. S., & Thimmiaraja, H. (2014). "Histogram Equalization for Image Enhancement Using MRI brain images", WCCCT, pp. 80 - 83.

Li, C., **Kao, C. Y., Gore, J. C. & Ding, Z.** (2008). Minimization of region-scalable fitting energy for image segmentation, Image Processing, IEEE Transactions on, vol. 17, no. 10, pp. 1940-1949.

Li, C., Huang, R., Ding, Z., Gatenby, J., Metaxas, D. N. & Gore, J. C. (2011). A level set method for image segmentation in the presence of intensity inhomogeneities with application to mri, Image Processing, IEEE Transactions on, vol. 20, no. 7, pp. 2007-2016.

Lin, G. C., **Wang, W. J., Kang, C.C. & Wang, C. M**. (2012). Multispectral mr images segmentation based on fuzzy knowledge and modified seeded region growing, Magnetic Resonance Imaging, vol. 30, no. 2, pp. 230-246.

Menze, B. H., **Van Leemput, K., Lashkari, D., Weber, M. A., Ayache, N. & Golland, P.** (2010). A generative model for brain tumor segmentation in multi-modal images, in Medical Image Computing and Computer-Assisted Intervention- MICCAI 2010. Springer, pp. 151-159.

Mitchell, T. M. (2006). The discipline of machine learning, Carnegie Mellon University, School of Computer Science.

Nie, J., **Xue, Z., Liu, T., Young, G. S., Setayesh, K., Guo, L. & Wong, S. T.** (2009). Automated brain tumor segmentation using spatial accuracy-weighted hidden markov random field, Computerized Medical Imaging and Graphics, vol. 33, no. 6, pp. 431-441.

Patel, A. & Mehta, K. (2012). "3D Modeling and Rendering of 2D Medical Image", International Conference on Communication Systems and Network Technologies, pp. 149 - 152.

Pham, D. L., **Xu, C. & Prince, J. L. (**2000**).** Current methods in medical image segmentation 1, Annual Review of Biomedical Engineering, vol. 2, no. 1, pp. 315-337.

Prastawa, M., **Bullitt, E., Ho. S. & Gerig, G.** (2004). A brain tumor segmentation framework based on outlier detection, Medical Image Analysis, vol. 8, no. 3, pp. 275-283.

Ruan, S., Lebonvallet, S., Merabet, A. & Constans, J. (2007). Tumor segmentation from a multispectral mri images by using support vector machine classification, in Biomedical Imaging: From Nano to Macro, 2007. ISBI 2007. 4th IEEE International Symposium on, IEEE, pp. 1236-1239.

Ruan, S., **Zhang, N., Liao, Q. & Zhu, Y.** (2011). Image fusion for following-up brain tumor evolution, in Biomedical Imaging: From Nano to Macro, 2011 IEEE International Symposium on, IEEE, pp. 281-284.

Sahar, M., **Nugroho, H. A., Tianur, A. I. & Choridah, L.** (2016). "Automated Detection of Breast Cancer Lesions Using Adaptive Thresholding and Morphological Operation", International Conference on Information Technology Systems and Innovation, pp.1 - 4.

Shiç F., **Yap, P.T., Fan, Y., Gilmore, J. H., Lin, W. & Shen, D.** (2010). Construction of multi-region-multi-reference atlases for neonatal brain mri segmentation, Neuroimage, vol. 51, no. 2, pp. 684-693.

Shenton, M., Kikinis, R., McCarley, W., Saiviroonporn, P., Hokama, H., Robatino, A., Metcalf, D., Wible, C., Portas, C. & Iosifescu, D. (1995). Harvard brain atlas: A teaching and visualization tool, in Proceedings of the 1995 Biomedical Visualization, pp. 10-17.

Stelldinger, P., Latecki, L. J. & Siqueira, M. (2007**).** "Topological Equivalence between a 3D Object and the Reconstruction of Its Digital Image", IEEE Transactions on Pattern Analysis and Machine Intelligence, pp. 126 - 140.

Subbanna, N. K., **Precup, D., Collins, D. L. & Arbel, T.** (2013). Hierarchical probabilistic gabor and mrf segmentation of brain tumours in mri volumes, in Medical Image Computing and Computer-Assisted Intervention-MICCAI 2013. Springer, pp. 751-758.

Szilagyi, L., **Benyo, Z., Szil´agyi, S. M. & Adam**, **H.** (2003). Mr brain image segmentation using an enhanced fuzzy cmeans algorithm, in Engineering in Medicine and Biology Society, 2003. Proceedings of the 25th Annual International Conference of the IEEE, IEEE, vol. 1, pp. 724-726.

Szilagyi, L., **Szil´agyi, S. M. & Benyo, Z.** (2007). A modified fuzzy c-means algorithm for mr brain image segmentation, in Image Analysis and Recognition. Springer, pp. 866-877.

Talairach, J. & Tournoux, P. (1988). Co-Planar Stereotaxic Atlas of the Human Brain: 3-dimensional proportation System an Approach to Cerebral Imaging. New York, USA: Thieme Medical Publishers.

Tran, T. N., **Wehrens, R. & Buydens, L.** (2005). Clustering multispectral images: A tutorial, Chemometrics and Intelligent Laboratory Systems, vol. 77, no. 1, pp. 3-17.

Verma, R., **Zacharaki, E. I., Ou, Y., Cai, H., Chawla, S., Lee, S. K., Melhem, E. R., Wolf, R. & Davatzikos, C.** (2008). Multiparametric tissue characterization of brain neoplasms and their recurrence using pattern classification of mr images, Academic Radiology, vol. 15, no. 8, pp. 966-977.

Weizmann, L., **Ben Sira, L., Joskowicz, L., Constantini, S., Precel, R., Shofty, B. & Ben Bashat, D.** (2012). Automatic segmentation, internal classification, and follow-up of optic pathway gliomas in mri, Medical Image Analysis, vol. 16, no. 1, pp. 177-188.

Zhang, N., Ruan, S., Lebonvallet, S., Liao, Q. & Zhu, Y. (2009). Multi-kernel SVM based classification for brain tumor segmentation of MRI multi-sequence, in Image Processing (ICIP), 2009 16th IEEE International Conference on, IEEE, pp. 3373-3376.

Zhang, N., **Ruan, S., Lebonvallet. S., Liao, Q. & Zhu, Y.** (2011). Kernel feature selection to fuse multi-spectral MRI images for brain tumor segmentation, Computer Vision and Image Understanding, vol. 115, no. 2, pp. 256-269.

Zhang, X., Li, X., Li, H. & Feng, Y. (2016). "A Semi – Automatic Brain Tumor Segmentation Algorithm", International Conference on Multimedia and Expo, pp. 1 - 6.

Zhou, J., Chan, K., Chong, V. & Krishnan, S. (2006). Extraction of brain tumor from mr images using one-class support vector machine, in Engineering in Medicine and Biology Society, 2005. IEEE-EMBS 2005. 27th Annual International Conference of the, IEEE, pp. 6411-6414.

Zikic, D., **Glocker, B., Konukoglu, E., Criminisi, A., Demiralp, C., Shotton, J., Thomas, O., Das, T., Jena, R. & Price, S.** (2012). Decision forests for tissue-specific segmentation of high-grade gliomas in multi-channel mr, in Medical Image Computing and Computer-Assisted Intervention-MICCAI 2012. Springer, pp. 369-376.